Excited-State Charge-Transfer Dynamics of Azurin, a Blue Copper Protein, from Resonance Raman Intensities

M. Adam Webb, Christine M. Kwong, and Glen R. Loppnow*

Department of Chemistry, University of Alberta, Edmonton, Alberta, Canada T6G 2G2

Received: December 18, 1996; In Final Form: April 8, 1997[⊗]

Resonance Raman spectra of azurin, a 14.6 kDa Type 1 blue copper protein from *Pseudomonas aeruginosa*, have been measured at wavelengths throughout the S(Cys) → Cu(II) charge-transfer absorption band centered at 625 nm in an effort to determine the role of environment and structure on the dynamics of excited-state charge transfer. Azurin provides an analogous system to plastocyanin, another Type 1 blue copper protein, whose excited-state structure and dynamics have been previously determined for a number of plant species. Self-consistent analysis of the absorption spectrum and the resulting resonance Raman excitation profiles using a time-dependent wave packet propagation formalism indicates that inhomogeneous effects account for the majority of the spectral broadening of the charge-transfer absorption band, in contrast to the primarily homogeneously broadened charge-transfer absorption band in plastocyanin. The total reorganization energy from the resonance Raman enhanced modes was found to be 0.26 ± 0.02 eV, compared to 0.19 ± 0.02 eV for plastocyanin. A detailed comparison of the copper environment in the two proteins reveals specific differences in structure and hydrogen-bonding environment which may explain the differences in observed excited-state charge-transfer dynamics of azurin and plastocyanin. The X-ray crystal structures of poplar *a* plastocyanin and *P. aeruginosa* azurin suggest that the larger coordination number accounts for the increased reorganization energy in azurin, and the increased hydrogen bonding at the copper site and/or conformational substates may explain the greater inhomogeneous component to the absorption line width in azurin.

Introduction

Blue copper proteins are involved in electron transport chains in plants and bacteria.[1,2] Azurin, a 14.6 kDa blue copper protein found in the denitrifying bacteria *Pseudomonas aeruginosa*, is involved in the electron transport chain of respiratory phosphorylation. Specifically, it transports electrons from cytochrome c_{551} to nitrite reductase (formerly called cytochrome oxidase).[1−3] The structure of azurin shows one Type I copper[4] ion in a coordination geometry which is an elongated, distorted trigonal bipyramid, with His46, Cys112, and His117 forming the three, strongly coordinated planar ligands, and Met121 and the carbonyl oxygen of Gly45 forming the weakly interacting axial ligands (Scheme 1). This is in contrast to plastocyanin, which exhibits a distorted tetrahedral geometry and has only one axial ligand, the sulfur of Met92.

The axial ligands in blue copper proteins seem to be responsible for tuning the copper ion EPR parameters, even though the bonds between these ligands and copper are typically quite long, 3.12 Å for Cu−S_{Met121} and 2.95 Å for Cu−O_{Gly45} in azurin.[5] Research performed on mutants of azurin,[6,7] in which the methionine ligand at amino acid 121 was replaced by a variety of amino acid residues or deleted completely, shows that the weakly bound S ligand has a significant effect on the copper coordination geometry. Replacing methionine with Leu, Ala, Val, Ile, or Trp results in an axial EPR spectrum, indicating a trigonal-planar geometry, weak or absent axial coordination, and a stronger interaction with the carbonyl oxygen. Replacing methionine with Asn, Asp, Gln, Cys, or His results in a rhombic EPR spectrum, indicating a more tetrahedral geometry and stronger axial coordination. In the latter mutants, the copper moves out of the NNS plane toward the now stronger axial ligand and away from the carbonyl oxygen.

SCHEME 1

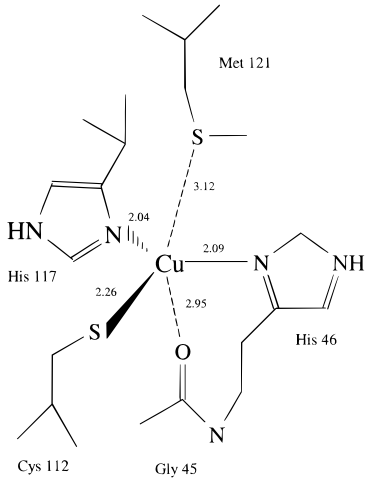

The redox potential also seems to be very sensitive to the number and type of axial ligands present. At pH 7.5, the reduction potentials of the copper site are +375 and +305 mV for plastocyanin and azurin, respectively.[1] These values are high compared to the aqua Cu(II/I) couple (+115 mV) and are characteristic of Type 1 copper proteins. The protein reduction potentials are pH dependent, and $E°$ values for all naturally occurring azurins are lower than those of plastocyanin.[8] By comparing azurin mutants, plastocyanin, and other blue copper proteins, it has been shown that the reduction potential increases as the copper moves further from the NNS plane toward the axial sulfur ligand, and the reduction potential decreases when the methionine ligand is removed.[6,8] These studies indicate that the interactions of the copper ion with the three strongly bound ligands remain fairly constant among azurin species while

* To whom correspondence should be addressed. E-mail: glen.loppnow@ualberta.ca; WWW: http://www.chem.ualberta.ca/~gloppnow.

⊗ Abstract published in *Advance ACS Abstracts,* June 1, 1997.

S1089-5647(97)00037-0 CCC: $14.00

variation in the axial ligands (distances and type) tunes the reduction potential.

The electronic structure of the copper site has been studied using low-temperature absorption, CD, and MCD spectroscopy[8−11] which have shown at least four transitions between 400 and 1000 nm. The most intense band has been assigned to a S(Cys-σ) → Cu charge-transfer transition, while the other transitions have been assigned to S(Cys-π) → Cu charge-transfer, S(Met-σ) → Cu charge-transfer, N(His-π) → Cu charge-transfer, and ligand field transitions. Studies using mutants and the addition of exogenous ligands show that the absorption spectrum is determined by the ligands coordinated to the copper ion.[6,12,13] As the copper site is altered from an axial Type 1 to a tetragonal Type 2 coordination structure, the absorption maxima at 460 and 628 nm are blue-shifted, and the peak at 460 nm grows in intensity at the expense of the 628 nm peak.[13] The substitution of a histidine with ligands that do not coordinate as well to the copper results in the blue-shifting of the 460 nm peak and the loss of the 625 nm peak.[13] Little mention is made in these studies regarding the altered nature of the electronic transitions.

The above studies all show that the protein is a significant factor in determining ground- and excited-state properties of blue copper proteins. In this paper, we examine the mode-specific nature of the protein's influence on the copper site properties with resonance Raman spectroscopy. Resonance Raman intensities provide detailed information about excited-state structure and dynamics on an extremely fast time scale.[14] Resonant enhancement of those normal modes coupled to the electronic transition occurs when the exciting laser is tuned to a wavelength within an absorption band.[14] Measurement of the resonance Raman intensity of each vibration as a function of excitation wavelength within an absorption band gives a set of resonance Raman excitation profiles. Self-consistent analysis of these resonance Raman excitation profiles and the absorption spectrum can yield such molecular parameters as the distortion along each normal mode upon photoexcitation, the homogeneous and inhomogeneous line widths, and transition moment.[14] In a charge-transfer absorption, resonance Raman intensities can also be used to partition the reorganization energy among the normal coordinates of the donor, acceptor, and solvent.[15−17]

In previous papers, we reported the use of resonance Raman and absorption spectroscopy to determine the mode-specific reorganization energies in a solute confined to a structurally well-defined solvent environment, specifically, the copper site in plastocyanins.[15,16] It was found that the reorganization energy of parsley plastocyanin is 0.19 eV along the resonance-enhanced Raman-active vibrations and 0.06 eV from a solventlike dephasing component due to the protein.[15] The dephasing component was deduced from the homogeneous line width needed to reproduce the resonance Raman cross section, after the term due to population relaxation was removed. The analysis indicated that the charge-transfer absorption band was primarily homogeneously broadened, as a result of fast (20 fs) population relaxation and protein-induced dephasing (15 fs).[15]

A similar analysis has been done for spinach and poplar *a* plastocyanin in order to examine the role of structure and environment on the excited-state charge-transfer process.[16] These two species gave values similar to parsley for many of the excited-state parameters such as the transition length, zero−zero energy, and homogeneous line width, reflecting the similar electronic nature of the excited states. A surprising result was that the resonance Raman spectra of the three species show modes of similar frequency, but have significant differences in relative intensities. The experimental resonance Raman frequencies and molecular modeling indicated that the copper site environment and the ground-state geometry are similar in the two plastocyanins, but that the reorganization energy is probably distributed differently among the normal modes. Comparison of the amino acid sequence in the three species using the experimentally determined structure of poplar *a* plastocyanin shows that these mode-specific excited-state changes occur as a result of an amino acid change ≥8 Å from the copper site.[16]

To better explore the relationship between protein composition, environment, and ground-state structure with excited-state structure and dynamics, we examine the excited-state charge-transfer dynamics in azurin with resonance Raman and absorption spectroscopy in this paper. The total, mode-specific, charge-transfer reorganization energy of 0.26 eV measured for azurin is significantly greater than the previously determined value of 0.19 ± 0.02 eV for the plastocyanins, probably indicating the effect of different coordination geometries in the two blue copper proteins. Partitioning of the spectral line shape into homogeneous and inhomogeneous components is also different, with azurin having a more significant inhomogeneous contribution to the total spectral line width than plastocyanin. The increased inhomogeneous line width probably arises from hydrogen bonding at the copper site and/or conformational substates present in azurin. These results show the ability of resonance Raman spectroscopy to distinguish the important structural and environmental determinants of excited-state charge-transfer dynamics.

Experimental Section

Preparation of azurin from *Pseudomonas aeruginosa* was based on a modification of literature procedures.[18−20] Briefly, cell cultures were grown anaerobically in 50 L batches and filtered. The resulting cell paste (typically 200 g) was either used immediately or frozen at −80 °C for later use. The cell paste was dried by using acetone, and the resulting powder was extracted with buffer (0.1 M ammonium acetate, pH 6.5). The solids were removed by centrifugation, and the supernatant was dialyzed against 0.05 M ammonium acetate (pH 4.0). The pH of the dialysate was adjusted to 4.0 and centrifuged. Azurin in the supernatant was oxidized by the addition of Na[Co(EDTA)] (∼1 mg/g of acetone powder) and purified by chromatography on CM-52 (Whatman), Sephadex G-50, and DE-52 (Whatman) columns. Additional G-50 and DE-52 columns were used to get a purity ratio (A_{280}/A_{625}) less than 2.1, close to the literature value of 1.7. A yield of 49−206 mg of azurin per 100 g of acetone powder was obtained using this method. The yield of azurin was found to be greatly dependent on the growth conditions of the bacteria; the yield was greatly reduced when the cells were overgrown.

Samples for the resonance Raman experiments were prepared by quantitative dilution of azurin with either a cacodylate/buffer solution (0.5−1.0 M cacodylic acid, 0.01 M TRIS-HCl, pH 8.7) or a nitrate/buffer solution (1.0 M potassium nitrate, 0.01 M TRIS-HCl, pH 8.7). Room-temperature resonance Raman spectra of azurin were obtained with 300 μL aqueous sample solutions (0.01 M TRIS-HCl buffer, either 0.375−0.8 M cacodylic acid or 0.8 M nitrate, pH 8.7) having an absorbance of 2.3−4.9 OD/cm at 625 nm ($\epsilon_{625} = 4800\ M^{-1}\ cm^{-1}$;[1,2,12] this is an average of the given literature values of 5200, 3500, and 5700 $M^{-1}\ cm^{-1}$, respectively). The addition of cacodylic acid/cacodylate buffer did not have a noticeable effect on the absorption or resonance Raman spectra of azurin. Resonance Raman scattering was excited by spherically focusing the laser onto a spinning 5 mm o.d. NMR tube containing the sample solution in a 135° backscattering geometry. Laser excitation was obtained with Kr ion (Coherent, Santa Clara, CA), CW

dye (Coherent), and HeNe lasers (PMS Electro-Optics, Boulder, CO). The wavelengths used were 530.9, 568.2, 647.1, and 676.4 nm (Kr^+), 589 and 614 nm (dye), and 594 and 612 nm (HeNe). The laser power was 100−130 mW (Kr^+, dye) or 7 mW (HeNe). Multichannel detection of resonance Raman scattering was obtained using a liquid nitrogen-cooled CCD detector (Princeton Instruments, Trenton, NJ) connected to the first half of a double monochromator (Spex Industries, Metuchen, NJ, Model 1401). Frequency calibration was performed by measuring Raman scattering of solvents of known frequencies (benzene, chloroform, carbon tetrachloride, and toluene). Frequencies are accurate to ± 2 cm^{-1}. Absorption spectra were recorded on a diode array spectrophotometer (Hewlett-Packard, Sunnyvale, CA, Model 8452A). Measurement of the resonance Raman spectrum and determination of the intensities were repeated on 3−6 fresh samples of azurin for each wavelength.

Analysis of the data was performed as previously described.[15] Bleaching of the sample was accounted for by measuring the absorbance at 580 nm ($\epsilon_{580} = 4494$ M^{-1} cm^{-1}) before and after each scan. The average absorbance was used to determine the concentration of azurin. The observed bleaching in a 90 min scan was <3%, suggesting that the bulk photoalteration parameter[21] is small. The single-pass photoalteration parameter was estimated using the following:

$$F = \frac{2.303 \times 10^3 \epsilon P \lambda t \phi}{N_A h c A} \tag{1}$$

where ϵ is the molar extinction coefficient at the excitation wavelength, P and λ are the power and wavelength of the laser, t is the average time a molecule spends in the laser beam, ϕ is the quantum yield for the process which causes photoalteration, and A is the $1/e^2$ area of the laser beam. At a wavelength of 568 nm and typical experimental conditions, a value for ϕ of 0.014 was calculated from the average bleaching of the samples. The average time a molecule spends in the beam was estimated from the laser beam diameter (1.0 mm) and the spin rate of the sample tube (100 Hz). The single-pass photoalteration parameter, F, was found to be 0.7%, which was deemed negligible.

Absolute resonance Raman cross sections were found from the relative integrated intensities using[22]

$$\sigma_{az} = \frac{I_{az}\left(\frac{1+\rho}{1+2\rho}\right)_{cac}[cac]S_{cac}}{I_{cac}\left(\frac{1+\rho}{1+2\rho}\right)_{az}[az]S_{az}}\sigma_{cac} \tag{2}$$

where I_{az} and I_{cac} are the integrated intensities of azurin and cacodylate, ρ is the depolarization ratio of the scattered light ($\rho_{az} = 0.33$ and $\rho_{cac} = 0.18$), [cac] and [az] are the concentrations of cacodylate and azurin, and S_{cac} and S_{az} are self-absorption correction factors for cacodylate and azurin. The correction for differential self-absorption at the azurin (S_{az}) and cacodylate (S_{cac}) frequencies was calculated using[23]

$$S_i = \frac{1 - \exp\left\{-\ln(10)\left(\frac{k_0}{\cos\theta} + k_i\right)b\right\}}{\ln(10)\left(\frac{k_0}{\cos\theta} + k_i\right)} \tag{3}$$

where $k_0 = \epsilon_{laser}c$, $k_i = \epsilon_i c$, c is the concentration of azurin, ϵ_{laser} and ϵ_i are the extinction coefficients at the laser and scattered wavelengths, respectively, $\theta = 45°$ is the incident angle of the laser with respect to the sample tube, and b is the sample path length. The differential self-absorption corrections between the cacodylate line and the azurin lines were less than 15%.

Absolute Raman cross sections for cacodylate, the internal intensity standard used, were measured at pH 8.7 and compared to previous measurements[15] at pH 7.6 to determine their pH dependence. Cross sections for cacodylate at pH 8.7 were measured by comparison with known values for nitrate[22] at 530.9, 568.2, 612, 647.1, and 676.4 nm, similar to that described previously.[15] The resulting experimental cacodylate cross sections were $(217 \pm 2) \times 10^{-14}$, $(125 \pm 6) \times 10^{-14}$, $(92.3 \pm 5.5) \times 10^{-14}$, $(63.7 \pm 2.4) \times 10^{-14}$, and $(68.9 \pm .4) \times 10^{-14}$ $Å^2$/molecule at 530.9, 568.2, 612, 647.1, and 676.4 nm, respectively. Because these experimental cross sections obtained at pH 8.7 were identical to those obtained at pH 7.6, the cacodylate cross sections used for the determination of absolute cross sections for azurin were 168×10^{-14}, 123×10^{-14}, 105×10^{-14}, 101×10^{-14}, 88.2×10^{-14}, 86.9×10^{-14}, 68.8×10^{-14}, and 56.6×10^{-14} $Å^2$/molecule at 530.9, 568.2, 589, 594, 612, 614, 647.1, and 676.4 nm, respectively, the same as those obtained previously.[15]

Theory

The resonance Raman and absorption cross sections in the Condon approximation can be written using the time-dependent equations of Lee and Heller.[14,15,24]

$$\sigma_R = \frac{8\pi E_S{}^3 E_L e^4 M^4}{9\hbar^6 c^4}\int_{-\infty}^{\infty} H(E_0)\,dE_0 \times \left|\int_0^{\infty}\langle f|i(t)\rangle e^{i(E_L+\epsilon_i)/\hbar}G(t)\,dt\right|^2 \tag{4}$$

$$\sigma_A = \frac{4\pi e^2 M^2 E_L}{6\hbar^2 cn}\int_{-\infty}^{\infty} H(E_0)\,dE_0 \int_{-\infty}^{\infty}\langle i|i(t)\rangle e^{i(E_L+\epsilon_i)/\hbar}G(t)\,dt \tag{5}$$

where E_L and E_S are the energies of the incident and scattered photons, M is the transition length, n is the refractive index, $H(E_0) = (1/[\theta(2\pi)^{1/2}])\exp[-(E_0 - \bar{E}_0)^2/2\theta^2]$ is a normalized Gaussian distribution of site electronic energies, ϵ_i is the energy of the initial vibrational state, $G(t)$ is a decay function, $|i\rangle$ and $|f\rangle$ are the initial and final vibrational wave functions in the resonance Raman process, and $|i(t)\rangle = e^{-iHt/\hbar}|i\rangle$ is the initial ground vibrational wave function propagated on the excited-state potential surface. The $\langle i|i(t)\rangle$ absorption overlap in eq 5 is the product of one-dimensional $\langle i|i(t)\rangle$ overlaps for each normal mode, while the $\langle f|i(t)\rangle$ Raman overlap in eq 4 is the product of $\langle f|i(t)\rangle$ along the Raman-active mode and $\langle i|i(t)\rangle$ along all other modes. In this treatment, the $\langle i|i(t)\rangle$ and $\langle f|i(t)\rangle$ overlaps are dependent only on the displacement, Δ, between ground- and excited-state equilibrium geometries along each normal coordinate. The implementation of these equations has been described in detail.[14−16,22] Self-consistent analysis of the absorption spectrum and the resonance Raman excitation profiles was done in the same manner as previously described for plastocyanin.[15,16]

Resonance Raman involves scattering of the incident photon from the excited electronic state. Because this process involves the excited electronic state, the intensities are sensitive to such excited-state parameters as the homogeneous and inhomogeneous line widths and changes in the equilibrium structure.[14−16] The homogeneous line width represents contributions from excited-state population decay and dephasing which occur on the time scale of the resonance Raman scattering, ~20 fs for azurin. As the homogeneous line width increases, the absorption spectrum broadens and becomes more diffuse. The resonance Raman excitation profiles also broaden and become more

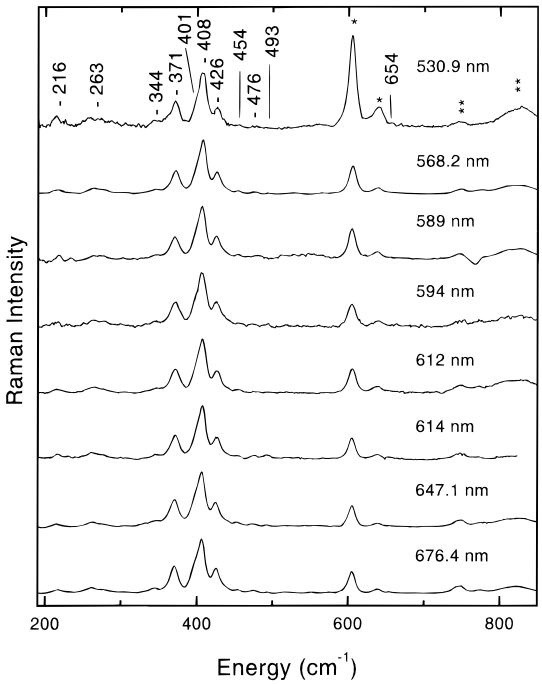

Figure 1. Resonance Raman spectra of azurin at excitation wavelengths throughout the 625 nm absorption band. The spectra are the sum of three to six scans. The vibrations between 200 and 500 cm^{-1} and the peak at 654 cm^{-1} were used in the analysis. Raman scattering of the internal intensity standard (cacodylate) is observed at 608 and 638 cm^{-1} (∗). The broad band at ∼820 cm^{-1} and the narrower band at 754 cm^{-1} (∗∗) are composed of the overtones and combinations of the azurin vibrations between 350 and 500 cm^{-1} and a cacodylate peak at 825 cm^{-1}.

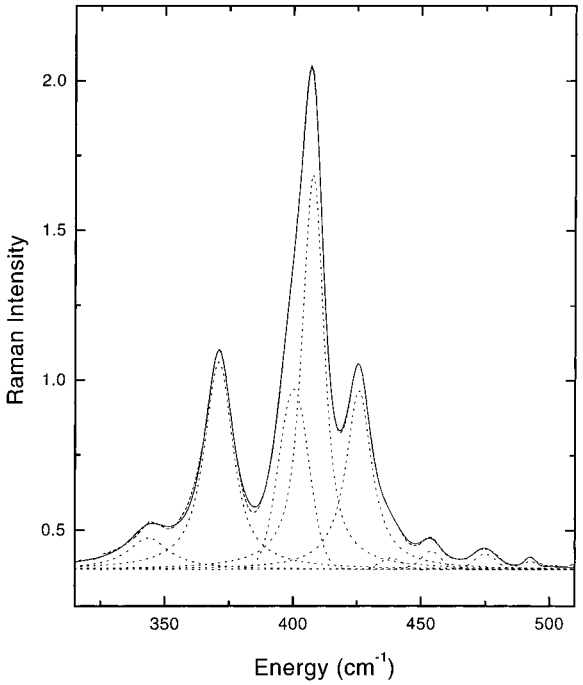

Figure 2. Deconvolution of the 300−500 cm^{-1} region of azurin. The solid curve is the sum of the individual peaks, shown as dotted lines. The experimental data is shown as a dashed line and is very closely overlapped by the fitted curve.

diffuse, but they also decrease in magnitude. The inhomogeneous line width is presumed to be due to probing an ensemble of molecules with different zero−zero energies which are considered to be static on the time scale of the resonance Raman scattering. The inhomogeneous line width affects both the absorption spectrum and the resonance Raman excitation profiles in a similar fashion; as the inhomogenous line width increases they both become broader and more diffuse, but the integrated intensity remains constant.

Results

The resonance Raman spectra of azurin at excitation wavelengths throughout the S(Cys) → Cu absorption band are shown in Figure 1. No reproducible peaks were observed at frequencies of less than 200 cm^{-1}; the single monochromator used to obtain the spectra was unable to separate the Rayleigh scattering from the low-frequency Raman signal. The intensity standard (cacodylate) appears at 605 and 638 cm^{-1}, marked with single asterisks in the figure. The intense bands between 340 and 440 cm^{-1} have been previously assigned to normal modes involving the Cu − S stretch mixed with other internal coordinates.[25−28] However, the exact assignments are still controversial.[25] The bands at 216 and 263 cm^{-1} have been assigned to modes involving the Cu−N stretches.[25] The broad band at about 830 cm^{-1}, marked by double asterisks in the figure, is due to combination and overtone bands of the vibrations between 340 and 440 cm^{-1}. There is also a contribution at 825 cm^{-1} from the As═O stretch of cacodylate.[29,30] Note in Figure 1 that the relative intensities of the azurin vibrations remain constant with respect to each other as the excitation wavelength is scanned through the absorption band. This indicates that all of the observed modes are coupled to a single electronic transition, namely, the S(Cys-σ) → Cu charge-transfer transition.

The depolarization ratios of azurin were measured at excitation wavelengths of 647.1 and 568.2 nm, on the red and blue edges of the putative S(Cys-σ) → Cu charge-transfer transition. The relative intensities of the azurin peaks did not change when the polarized spectra were measured, indicating that all the azurin modes have identical polarization ratios. The depolarization ratios were found to be 0.40 ± 0.08, independent of wavelength. This is consistent with there being only a single electronic transition which enhances the Raman scattering.

Figure 2 shows the deconvolution of the observed bands into individual vibrational transitions. The frequencies of the resulting peaks correspond well to those previously reported at low temperature, at which the bands are better resolved.[25] Note that the deconvolved peaks all have approximately the same line width, suggesting that they are an accurate reflection of the individual transitions. For the deconvolution of all spectra in this paper, the positions, widths, and shapes of the component peaks were kept constant; only the heights were allowed to vary to obtain an optimum fit to the observed spectrum.

The experimental and calculated absolute resonance Raman cross sections are summarized in Table 1. Figures 3 and 4 show the good agreement of the experimental and calculated absorption spectra and resonance Raman excitation profiles. The parameters used for the calculated curves are given in Table 1. Deviations of the experimental absorption spectra from the calculated absorption spectrum at both higher and lower energies are due to the presence of other charge-transfer and ligand field transitions which were not modeled and apparently contribute no resonance enhancement to the observed normal modes (see above). The resonance Raman excitation profiles have a maximum intensity at ∼610 nm which is significantly blue-shifted from the absorption maximum of 628 nm and are also narrower than the absorption band. These two results are consistent with there being more than one electronic transition within the absorption band. Due to the presence of more than one electronic transition within the charge-transfer absorption band, the resonance Raman excitation profiles provided the primary constraints on the simulated spectral band shape and

TABLE 1: Absolute Resonance Raman Cross Sections of Azurin[a]

		excitation wavelength/nm							
$\Delta\nu$/cm^{-1}	$\|\Delta\|$	530	568.2	589	594.0	612	614	647	676.4
216	0.85	0.53/0.12	0.61/0.51	0.83/0.82	−/0.88	1.22/1.03	0.63/1.04	0.68/0.78	0.47/0.34
263	1.26	1.07/0.40	1.30/1.67	1.81/2.68	3.33/2.87	2.96/3.30	2.73/3.31	1.56/2.42	1.06/1.05
344	0.75	0.50/0.26	0.99/1.04	1.37/1.63	1.86/1.74	1.90/1.95	1.93/1.95	1.42/1.36	0.95/0.57
371	1.60	1.71/1.45	4.64/5.65	7.05/8.66	9.39/9.18	9.12/10.1	10.3/10.0	6.29/6.80	4.52/2.79
401	1.22	1.04/0.96	3.08/3.81	5.89/5.90	6.87/6.26	6.33/6.94	6.95/6.92	4.53/4.71	3.28/1.94
408	1.64	2.38/1.80	6.79/7.15	9.14/11.0	12.0/11.7	12.2/13.0	13.6/12.9	7.01/8.76	4.73/3.60
426	1.26	1.18/1.17	3.91/4.63	5.03/7.12	8.36/7.54	7.39/8.30	8.24/8.29	4.98/5.57	3.54/2.27
439	0.23	0.01/0.04	0.14/0.16	0.32/0.25	−/0.27	0.24/0.29	0.29/0.29	0.18/0.20	0.14/0.08
454	0.31	0.07/0.08	0.28/0.31	0.54/0.47	0.53/0.50	0.51/0.55	0.45/0.55	0.49/0.36	0.23/0.15
476	0.27	0.06/0.07	0.21/0.27	−/0.41	0.46/0.43	−/0.47	−/0.47	0.28/0.31	0.21/0.12
493	0.13	−/0.02	0.06/0.07	−/0.10	−/0.11	−/0.12	−/0.12	0.06/0.08	0.04/0.03
654	0.18	0.14/0.06	0.19/0.24	0.05/0.34	−/0.36	0.33/0.37	0.37/0.37	0.30/0.23	0.16/0.08

[a] The resonance Raman cross sections are shown as experimental/calculated in units of Å^2/molecule × 10^{10}. A − indicates no signal was observed above the baseline noise and no cross section was measured. The errors in cross sections are ±10% for strong lines and ±20% for weak lines. The Δ's are in dimensionless normal coordinates. The cross sections were calculated with eq 4 using the following parameters: zero−zero energy, $E_0 = 14\,200$ cm^{-1}, transition length, $M = 0.63$ Å, temperature, $T = 0$ K, refractive index, $n = 1.33$, Lorentzian homogeneous line width, $\Gamma = 160$ cm^{-1}, inhomogeneous line width, $\Theta = 280$ cm^{-1}.

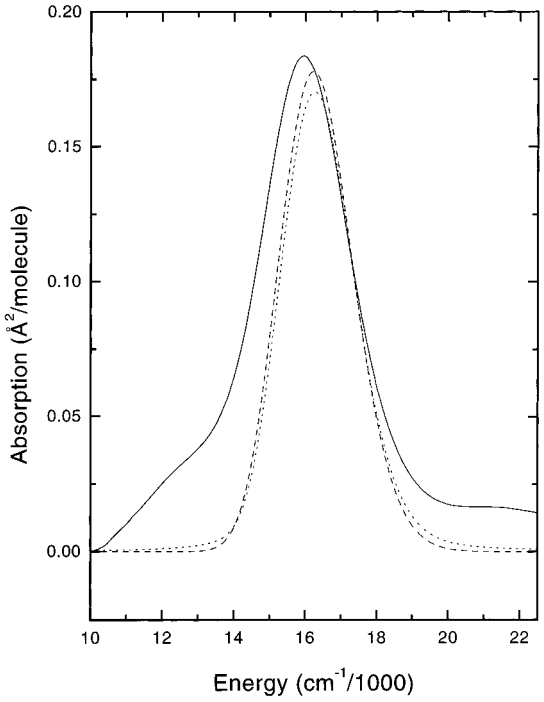

Figure 3. Experimental (solid line) and calculated (dashed/dotted lines) absorption spectra of azurin. The dotted line was calculated using a Lorenztian homogeneous line shape, and the dashed line was calculated using a Gaussian homogeneous line shape. Deviations of the experimental absorption spectrum from the calculated absorption spectra at both higher and lower energies are due to the presence of other charge-transfer and ligand field transitions which were not modeled and apparently contribute no resonance enhancement to the observed normal modes. Note the better reproduction of the blue edge of the absorption spectrum with the Lorentzian line shape.

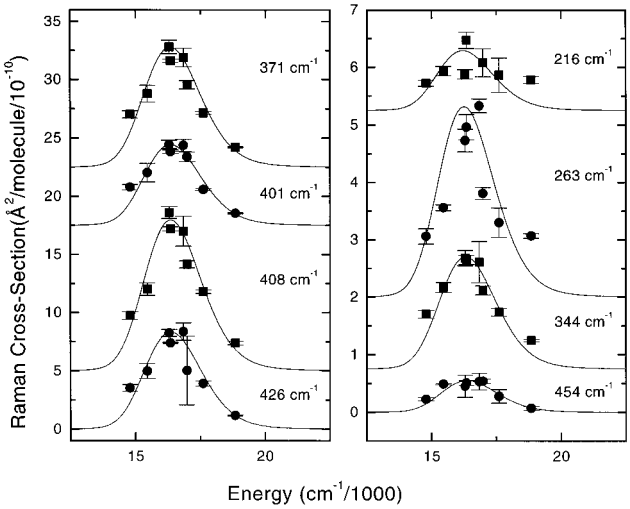

Figure 4. Experimental (points) and calculated (solid line) resonance Raman excitation profiles of azurin. The excitation profiles were calculated with eq 4 using the parameters in Table 1. Note the difference in scale between the left and right panels.

bandwidth. Thus, scaling of the Δ's was determined by the width of the resonance Raman excitation profiles. In the simulations, it was necessary to use significant amounts of inhomogeneous broadening, in addition to homogeneous broadening, to reproduce the large resonance Raman cross sections and diffuse absorption band. Figure 3 shows the best fit using a Gaussian (dashed line) and Lorentzian (dotted line) line shape to model the absorption spectrum. A Lorentzian homogeneous function was found to fit the shape of the absorption band better than a Gaussian function, although the band shape was underconstrained by the experimental data. The molecular mechanism of these different line shapes is discussed below.

The intensity of the overtone and combination bands was measured at 647.1 nm using nitrate as the internal standard (0.8 M nitrate, 0.01 M TRIS-HCl, pH 8.7) as a check on the resonance Raman intensity analysis (Figure 5). Measurement of the overtone and combination band intensities provides an additional constraint on the excited-state frequencies assumed in the calculations. The nitrate peak appears at 1049 cm^{-1} and is marked with an asterisk in the figure. The bands in this region have been assigned[25] to a C−S fundamental band at 753 cm^{-1} and various overtone and combination bands from 740 to 900 cm^{-1} arising from the intense mode at 408 cm^{-1}. The fundamental band at 753 cm^{-1} is overlapped by the overtone of the 371 cm^{-1} mode at 742 cm^{-1} and appears as one peak at ∼749 cm^{-1}. Because the resonance Raman spectra were taken at room temperature, we were unable to resolve the overtone and combination bands into individual vibrational transitions. Small peaks were observed at frequencies greater than 900 cm^{-1} (marked with **). However, these bands were not reproducible in either intensity or position and so were not used for this analysis. The overall intensity of the overtone region from 760 to 900 cm^{-1} was calculated to be 7.58×10^{-10} cm^2/molecule, using eq 4 and the parameters in Table 1, which is in agreement with the measured value of 5.97×10^{-10} cm^2/molecule, within experimental error. The band at ∼749 cm^{-1} was not used in

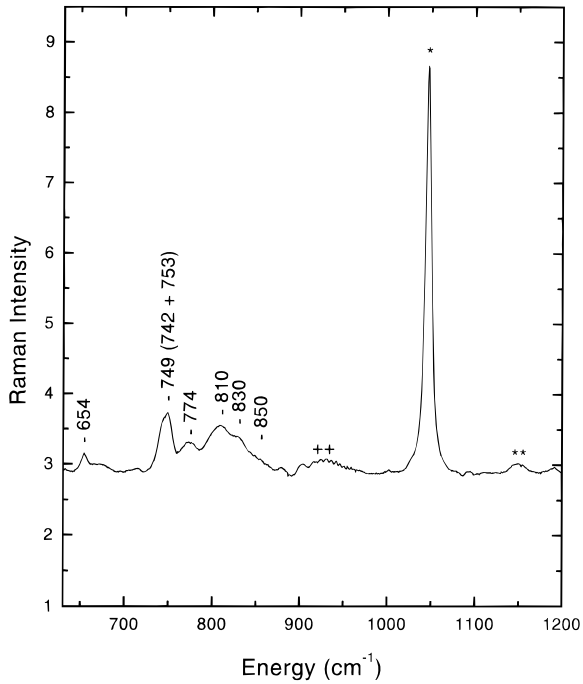

Figure 5. Resonance Raman spectra of azurin overtone and combination bands using an excitation wavelength of 647.1 nm. The spectrum is the sum of three scans. Raman scattering of the internal standard (nitrate) is observed at 1049 cm^{-1} (∗). Small peaks were observed at ∼1150−1200 cm^{-1} (∗∗) which were not reproducible. The feature at ∼950 cm^{-1} (++) is an artifact of the CCD detector.

TABLE 2: Comparison of the Excited-State Charge-Transfer Parameters for Azurin and Plastocyanin[a]

	azurin[b]	plastocyanin[c]
E_0 (cm^{-1})	14200 ± 140	15350 ± 150
M (Å)	0.63 ± 0.01	0.581 ± 0.01
Θ (cm^{-1})	280 ± 14	0
Γ_G (cm^{-1})	0	385 ± 19
Γ_L (cm^{-1})	160 ± 8	0

[a] In this table, E_0 is the zero−zero energy, M is the transition length, Θ is the inhomogeneous line width, and Γ_G and Γ_L are the Gaussian and Lorentzian homogeneous line widths, respectively. [b] Values from this work. [c] Values from ref 15.

comparing the calculations and experimental data, as it has been assigned[25] to an overlap of an overtone (743 cm^{-1}) and a fundamental (753 cm^{-1}) and we were unable to resolve them.

Discussion

Comparison to Plastocyanin. The primary goal of this work is to determine the role of structure and environment on the dynamics of excited-state charge transfer. This has been done previously for a series of plastocyanins in which the structure and environment were not significantly different near the copper site, in order to explore the effects of remote differences (i.e., at distances ≥8 Å).[16] In this section, a comparison of the excited-state charge-transfer dynamics in plastocyanin and azurin is performed to examine the role of coordination geometry and hydrogen bonding in the immediate vicinity of the copper site.

A comparison of the excited-state parameters of azurin and plastocyanin is shown in Table 2. The zero−zero energy, E_0, and the transition length, M, of azurin are both found to be different than those of plastocyanin. These differences can be attributed to structural differences around the copper metal center. The transition length of azurin is 0.05 Å larger than that of plastocyanin, which is close to the 0.13 Å difference in the Cu−S(Cys) bond length between the two proteins from X-ray crystallography.[5,31] This result suggests that roughly the same amount of charge is transferred in the two proteins. Apparently, the coupling between the copper and sulfur is strong enough that the transition dipole qualitatively increases with increasing distance between donor and acceptor. The zero−zero energy of azurin is found to be 1150 cm^{-1} lower than that of plastocyanin, which is consistent with the observed 750 cm^{-1} shift of the absorption band maximum of azurin to lower energy. The additional 400 cm^{-1} shift is due to the greater Δ's in azurin (see below).

The absorption band of plastocyanin was found to be primarily homogeneously broadened, in contrast to azurin which has significant inhomogeneous broadening. Plastocyanin was found to have a total phenomenological Gaussian homogeneous line width of 385 cm^{-1} while azurin has a mixture of Lorentzian homogeneous (160 cm^{-1}) and Gaussian inhomogeneous line widths (280 cm^{-1}). This difference in partitioning of the broadening among homogeneous and inhomogeneous components is real and is probably due to environmental differences in the two proteins. It has been suggested that azurin has three conformational substates from the multiexponential fluorescence decay of Trp48.[32−34] Similar studies have not been done on plastocyanin. Fluctuations between these conformational substates can contribute to the inhomogeneous and homogeneous broadening depending on the time scale of the fluctuations. The resonance Raman scattering occurs within the total optical dephasing time of ∼30 fs, as determined here by the homogeneous line width. This is on the order of a vibrational period for a high-frequency mode (∼1000 cm^{-1}), much higher than would be expected for global conformational changes in the protein. Therefore, we expect conformational substates to contribute to the inhomogeneous line width (i.e., the protein should be static on the time scale of resonance Raman scattering). An additional factor in the broadening mechanism is the role of the hydrogen-bonding environment. In azurin and plastocyanin the orientation of the ligands are tightly constrained by the surrounding protein structure.[4,31] In both proteins, five hydrogen bonds, including a hydrogen bond between an Asn (azurin, Asn47; plastocyanin, Asn38) and the metal-coordinating Cys, determine the shape of the protein folding in the region of the metal center and the separation of histidine and cysteine. However, azurin also contains a second hydrogen bond between the peptide NH of Phe114 and the metal-coordinating Cys, whereas this Cys in plastocyanin has only the Cys−Asn hydrogen bond. This additional hydrogen bond in azurin may increase the inhomogeneous broadening in the S(Cys-σ) → Cu charge-transfer absorption.

Although we attempted to measure the fluorescence spectrum of azurin, no detectable fluorescence was observed at energies above 13 500 cm^{-1}, the lower limit of our detection system (data not shown). Taking three times the standard deviation of the noise observed in an earlier measurement of the fluorescence of plastocyanin[15] as the minimum measurable signal gives a lower detection limit of $\Phi_F = 1 \times 10^{-7}$. We may not have observed a fluorescence signal because the fluorescence spectrum may be shifted to lower energies than we were able to detect. The absorption maximum of azurin is shifted 750 cm^{-1} to lower energies than that of plastocyanin. If the fluorescence maximum is shifted by the same amount from the observed fluorescence maximum of plastocyanin, the expected fluorescence maximum for azurin would be approximately 13 250 cm^{-1}. If the plastocyanin fluorescence signal is shifted 750 cm^{-1} to the red, we should still be able to observe the blue edge of the fluorescence band, within the noise limit described above. However, this assumes the Stokes shifts in the two

TABLE 3: Mode-Specific Reorganization Energies of Azurin and Plastocyanin[a]

azurin[b]			plastocyanin[c]		
$\Delta\nu$/cm^{-1}	$\|\Delta\|$	λ/cm^{-1}	$\Delta\nu$/cm^{-1}	$\|\Delta\|$	λ/cm^{-1}
216	0.85	78			
263	1.30	220	266	0.98	130
344	0.75	100			
371	1.60	470	376	1.40	370
401	1.20	290	390	1.20	280
408	1.60	520	403	0.49	48
426	1.30	360	421	1.40	410
439	0.23	12	436	0.98	210
454	0.31	22			
476	0.27	17	473	0.24	14
493	0.13	4			
654	0.18	11			
			759	0.35	46
total		2100			1500

[a] Δ's are in dimensionless normal coordinates. The reorganization energy in a particular mode, λ_i, is related to Δ_i by $\lambda_i = (\Delta_i^2\omega_i)/2$ where ω_i is the frequency in cm^{-1}. [b] Values for azurin from this work. [c] Values for plastocyanin from ref 15.

proteins are the same. The Stokes shift for azurin is expected to be larger due to the larger Δ's, resulting in the fluorescence being shifted to even lower energies than predicted from the observed absorption band shift. By comparing the difference in the zero−zero energy (1150 cm^{-1}) of the two proteins, the increase in Stokes shift is about 400 cm^{-1} in azurin. This would shift the fluorescence maximum of azurin to 12 800 cm^{-1}, compared to ∼14 000 cm^{-1} for plastocyanin. With the fluorescence shifted so far to the red, we would not expect to see any fluorescence from azurin within our experimental detection limit.

Reorganization Energy. Comparison of the mode-specific reorganization energies in azurin and plastocyanin reveals some interesting similarities and differences. Table 3 compares the resonance Raman frequencies and mode-specific reorganization energies, as calculated from the observed Δ's, of azurin and plastocyanin. In both proteins the majority of the resonance Raman intensity is in bands between 300 and 450 cm^{-1}. These bands have been assigned to the Cu−S(Cys) stretch coupled to other internal coordinates.[25] Most (85%) of the reorganization energy in azurin occurs in modes between 300 and 500 cm^{-1}. This is similar to plastocyanin, in which modes between 350 and 500 cm^{-1} contribute 90% of the reorganization energy, although it appears to be spread over fewer modes in plastocyanin. Smaller contributions (15%) to the reorganization energy in azurin are made by the modes at 216, 263, and 654 cm^{-1}. A number of modes of azurin and plastocyanin have similar frequencies (Table 3). This is expected, since the resonance Raman spectra of 11 blue copper proteins all show vibrational modes between 350 and 500 cm^{-1}, albeit with different relative intensities.[3] However, the reorganization energy in the two proteins is significantly different along modes with similar frequencies, reflected in the very different absolute resonance Raman cross sections, with those of azurin often being substantially higher than those of plastocyanin. The total reorganization energy from all of the observed Raman modes is significantly larger in azurin than in plastocyanin (0.26 eV compared to 0.19 eV). For modes of similar frequency, azurin generally has greater reorganization energy. For example, the reorganization energy for the 408 (403) cm^{-1} mode of azurin (plastocyanin) is 520 (48) cm^{-1}. An exception to this observation is the 439 (436) cm^{-1} mode of azurin (plastocyanin) in which the reorganization energy is 12 (210) cm^{-1} for azurin (plastocyanin). The greater total reorganization energy in azurin is expected, as there is an additional ligand bound to the copper in azurin. Increasing the number of atoms in the coordination sphere is expected to increase the number of vibrational modes and the total reorganization energy, since it generally takes more energy to reorganize the nuclei of five ligands than four upon charge transfer. If we assume that the reorganization energy is proportional to the number of atoms directly ligated to the copper ion, we would predict that azurin would have a reorganization energy of 0.19 eV × 5/4 = 0.24 eV compared to plastocyanin. This is close to the value of 0.26 eV that is observed experimentally. Increased reorganization in azurin may also indicate that the vibrational modes are more strongly coupled to the charge transfer than those of plastocyanin. Stronger coupling would result in larger displacements of the modes in the charge-transfer excited state and therefore a higher reorganization energy. A possible explanation of stronger coupling in azurin is the stiffness of the copper site. Studies of the X-ray crystal structure of the apoprotein suggest that the protein determines the coordination geometry at the copper site.[35−37] Structural changes at the copper site could induce structural changes to the protein backbone and affect side-chain vibrations coupled to the local motions. The metal center of azurin is expected to be more rigid than that of plastocyanin due to an additional copper coordination bond to a carbonyl group and an additional hydrogen bond between Cys and the backbone NH of Phe114. Increased rigidity of the copper site would increase the mechanical coupling to the protein backbone and increase coupling to local motions.

The calculated reorganization energy can be compared to the upper limit reorganization enthalpy at the copper site of 0.3 eV measured for electron transport,[38] corresponding to a reorganization energy of 1.2 eV. However, this reorganization energy is measured for the process in which one electron is transferred. Assuming that the reorganization energy scales approximately linearly with the amount of charge transferred and using the value of ∼25% of a charge shift between the ground and excited state,[39] we suggest that the total, mode-specific reorganization energy measured here of 0.26 eV is in good agreement with the upper limit value of 0.3 eV.[38]

In plastocyanin, a Brownian oscillator model was used to represent the contribution of the solvent environment to the homogeneous line width[40,41] where $G(t) = \exp\{-g(t)\}$, $g(t) = g_R(t) + ig_I(t)$, and

$$g_R(t) = (D^2/\Lambda^2)[\exp(-\Lambda t/\hbar) - 1 + \Lambda t/\hbar] \quad (6a)$$

$$g_I(t) = (D^2/2kT\Lambda)[1 - \exp(-\Lambda t/\hbar)] \quad (6b)$$

In this model D is the coupling strength between the electronic and solvation coordinates, $\hbar/\Lambda$ is the characteristic time of the solvation modulation, and the solvent reorganization energy is $D^2/2kT$. A Lorenztian line width of 160 cm^{-1} can be approximately modeled using eqs 6a and 6b with D = 630 cm^{-1} and Λ = 2400 cm^{-1}, yielding a solvent reorganization energy of 0.12 eV. This is twice the 0.06 eV which was determined for plastocyanin.[15] This suggests that the solvent reorganization energy of azurin may be greater than that of plastocyanin. However, the above calculation neglects population decay and assumes that the entire line width is due to solvent-induced dephasing. Because the population decay rate has not been measured for azurin, a direct comparison is difficult.

Normal Modes. This analysis provides a quantitative measurement of the reorganization energy along each resonance

Raman-active mode. A normal coordinate analysis is necessary to determine the contributions of each internal coordinate (i.e., stretch, bend, etc., of individual bonds) to the reorganization energy. This analysis is important to perform since the observed differences in the resonance Raman intensity pattern and mode-specific reorganization energies of the two proteins may be due to differences in the normal mode descriptions. A normal coordinate analysis is difficult to complete for azurin and plastocyanin due to the difficulty in preparing isotopic derivatives and the lack of model compounds that have similar electronic and vibrational properties. However, some information has recently become available for the normal mode description of blue copper proteins. Recently, some resonance Raman spectra have been reported for isotopically substituted azurin,[26] plastocyanin,[28] and a model compound[42] with similar electronic and vibrational properties to blue copper proteins. These studies suggest that the Cu−S internal coordinate is highly coupled to bending coordinates of Cys112 to form the normal modes grouped between 340 and 500 cm^{-1}. In this picture, the resonance-enhanced normal modes arise from internal coordinates localized on the immediate coordination ligands. However, a normal coordinate analysis based on the crystallographic structure with a number of simplifications has been done on 169 atoms around the copper metal site in three Type 1 copper proteins[43] and predicts that protein motions far from the copper site may be coupled to the resonance-enhanced normal modes. This theoretical model was supported by a recent study of the resonance Raman intensities for a homologous series of plastocyanins[16] that found that significant changes in reorganization energy along specific normal modes occur for plastocyanins which have identical structures and amino acid compositions up to 8 Å from the copper site. This study suggests that protein vibrations far from the copper site are coupled to the local motions such as the Cu−S(Cys) stretch in plastocyanin. If this is the case, the normal mode descriptions of azurin and plastocyanin are expected to be quite different as the amino acid compositions differ significantly further from the copper center.

Conclusions

There are two main results of this work. First, the resonance Raman spectrum and charge-transfer reorganization energies of azurin have some qualitative similarities to plastocyanin. In the photoexcited charge-transfer process, most of the reorganization energy occurs along the putative Cu−S(Cys) stretch, and the frequencies of the modes are similar in the two proteins. The absorption spectra are also similar in shape, although the absorption maximum of azurin is shifted to lower energy. Second, the structure and environment around the copper metal ion have a significant and quantitative role in determining the electronic structure and excited-state dynamics. Differences in the excited-state photophysical charge-transfer parameters of plastocyanin and azurin, such as the homogeneous and inhomogeneous line widths, zero−zero energy, transition moment, and reorganization energy, can be related to specific structural factors such as the coordination geometry of the copper center and the hydrogen-bonding environment.

Acknowledgment. We thank Dr. T. Harris, Dr. K. Michaelian, Prof. M. Palcic, Prof. H. B. Dunford, and Prof. N. Dovichi for equipment support. We also thank R. Mah and Prof. M. Pickard at the University of Alberta for the growth and harvesting of *P. aeruginosa*. Financial support was provided by NSERC and the Alberta Heritage Foundation for Medical Research.

References and Notes

(1) Sykes, A. G. *Adv. Inorg. Chem.* **1991**, *36*, 377.

(2) Adman, E. T. In *Metalloproteins—Part 1: Metal Proteins with Redox Roles*; Harrison, P. M., Ed.; Verlag Chemie: New York, 1985; p 1.

(3) Adman, E. T. *Adv. Protein Chem.* **1991**, *42*, 145.

(4) Baker, E. N. *J. Mol. Biol.* **1988**, *203*, 1071.

(5) Nar, H.; Messerschmidt, A.; Huber, R.; van de Kamp, M.; Canters, G. W. *J. Mol. Biol.* **1991**, *221*, 765.

(6) Murphy, L. M.; Strange, R. W.; Karlsson, B. G.; Lungburg, L. G.; Pascher, T.; Reinhammar, B.; Hasnain, S. S. *Biochemistry* **1993**, *32*, 1965.

(7) Karlsson, B. G.; Nordling, M.; Pascher, T.; Tsai, L.-C.; Sjölin, L.; Lundberg, L. G. *Protein Eng.* **1991**, *4*, 343.

(8) Ainscough, E. W.; Bingham, A. G.; Brodie, A. M.; Ellis, W. R.; Gray, H. B.; Loehr, T. M.; Plowman, J. E.; Norris, G. E.; Baker, E. N. *Biochemistry* **1987**, *26*, 71.

(9) Solomon, E. I.; Hare, J. W.; Gray, H. B. *Proc. Natl. Acad. Sci. U.S.A.* **1976**, *73*, 1389.

(10) Solomon, E. I.; Hare, J. W.; Dooley, D. M.; Dawson, J. H.; Stephens, P. J.; Gray, H. B. *J. Am. Chem. Soc.* **1980**, *102*, 168.

(11) Tang, S.-P. W.; Coleman, J. E.; Myer, Y. P. *J. Biol. Chem.* **1968**, *243*, 4286.

(12) den Blaauwen, T.; Canters, G. W. *J. Am. Chem. Soc.* **1993**, *115*, 1121.

(13) Andrew, C. R.; Yeom, H.; Valentine, J. S.; Karlsson, B. G.; Bonander, N.; van Pouderoyen, G.; Canters, G. W.; Loehr, T. M.; Sanders-Loehr, J. *J. Am. Chem. Soc.* **1994**, *116*, 11489.

(14) Myers, A. B.; Mathies, R. A. In *Biological Applications of Raman Spectroscopy*; Spiro, T. G., Ed.; Wiley: New York, 1988; Vol. 2, p 1.

(15) Fraga, E.; Webb, M. A.; Loppnow, G. R. *J. Phys. Chem.* **1996**, *100*, 3278.

(16) Loppnow, G. R.; Fraga, E. *J. Am. Chem. Soc.* **1997**, *119*, 896.

(17) Myers, A. B. *Chem. Rev.* **1996**, *96*, 911.

(18) St. Clair, C. S.; Ellis, W. R. J.; Gray, H. B. *Inorg. Chim. Acta* **1992**, *191*, 149.

(19) Ambler, R. P. *Biochem. J.* **1963**, *89*, 341.

(20) Ambler, R. P.; Wynn, M. *Biochem. J.* **1973**, *131*, 485.

(21) Mathies, R. A.; Oseroff, A. R.; Stryer, L. *Proc. Natl. Acad. Sci. U.S.A.* **1976**, *73*, 1.

(22) Loppnow, G. R.; Mathies, R. A. *Biophys. J.* **1988**, *54*, 35.

(23) Womack, J. D.; Mann, C. K.; Vickers, T. J. *J. Appl. Spectrosc.* **1989**, *43*, 527.

(24) Lee, S.-Y.; Heller, E. J. *J. Chem. Phys.* **1979**, *71*, 4777.

(25) Blair, D. F.; Campbell, G. W.; Schoonover, J. R.; Chan, S. I.; Gray, H. B.; Malmstrom, B. G.; Pecht, I.; Swanson, B. I.; Woodruff, W. H.; Cho, W. K.; English, A. M.; Fry, H. A.; Lum, V.; Norton, K. A. *J. Am. Chem. Soc.* **1985**, *107*, 5755.

(26) Dave, B. C.; Germanas, J. P.; Czernuszewicz, R. S. *J. Am. Chem. Soc.* **1993**, *115*, 12175.

(27) Han, J.; Loehr, T. M.; Lu, Y.; Valentine, J. S.; Averill, B. A.; Sanders-Loehr, J. *J. Am. Chem. Soc.* **1993**, *115*, 4256.

(28) Qiu, D.; Dong, S.; Ybe, J. A.; Hecht, M. H.; Spiro, T. G. *J. Am. Chem. Soc.* **1995**, *117*, 6443.

(29) Grundler, H.; Schumann, H. D.; Steger, E. *J. Mol. Struct.* **1974**, *21*, 149.

(30) Vansant, F. K.; van der Veken, B. J.; Herman, M. A. *Spectrochim. Acta* **1974**, *30A*, 69.

(31) Guss, J. M.; Freeman, H. C. *J. Mol. Biol.* **1983**, *169*, 521.

(32) Ehrenstein, D.; Nienhaus, G. U. *Proc. Natl. Acad. Sci. U.S.A.* **1992**, *89*, 9681.

(33) Hutnik, C. M.; Szabo, A. G. *Biochemistry* **1989**, *28*, 3923.

(34) Hutnik, C. M.; Szabo, A. G. *Biochemistry* **1989**, *28*, 3935.

(35) Garrett, T. P. J.; Clingeleffer, D. J.; Guss, J. M.; Rogers, S. J.; Freeman, H. C. *J. Biol. Chem.* **1984**, *259*, 2822.

(36) Nar, H.; Messerschmidt, A.; Huber, R.; van de Kamp, M.; Canters, G. W. *FEBS Lett.* **1992**, *306*, 119.

(37) Shepard, W. E. B.; Kingston, R. L.; Anderson, B. F.; Baker, E. N. *Acta Crystallogr.* **1993**, *49D*, 331.

(38) Margalit, R.; Kostic, N. M.; Che, C.-M.; Blair, D. F.; Chiang, H.-J.; Pecht, I.; Shelton, J. B.; Shelton, J. R.; Schroeder, W. A.; Gray, H. B. *Proc. Natl. Acad. Sci. U.S.A.* **1984**, *81*, 6554.

(39) Solomon, E. I.; Lowery, M. D. *Science* **1993**, *259*, 1575.

(40) Bosma, W. B.; Yan, Y. J.; Mukamel, S. *Phys. Rev. A* **1990**, *42*, 6920.

(41) Mukamel, S. *Annu. Rev. Phys. Chem.* **1990**, *41*, 647.

(42) Qiu, D.; Kilpatrick, L.; Kitajima, N.; Spiro, T. G. *J. Am. Chem. Soc.* **1994**, *116*, 2585.

(43) Urushiyama, A.; Tobari, J. *Bull. Chem. Soc. Jpn.* **1990**, *63*, 1563.